EFFECT OF ELASTIC INTERACTION ENERGY ON THE DISTRIBUTION OF COHERENT PRECIPITATE PARTICLES IN NICKEL-BASE ALLOYS

Minoru Doi and Toru Miyazaki

Department of Materials Science and Engineering
Metals Section, Nagoya Institute of Technology
Gokiso-cho, Showa-ku, Nagoya 466, Japan

Abstract

Two new parameters which can numerically describe the precipitate distribution are proposed. One is for the directional alignment along [*hkl*] direction and is symbolized by Ψ_{hkl}. The other is for the non-uniform (localized) distribution and is symbolized by Λ. By using the parameters, the sequence of morphological change of coherent precipitates under the influence of elastic interaction energy in Ni-base alloys are analyzed and the following conclusions are obtained: (1) as coarsening proceeds, the alignment along <100> starts, then the localization also starts, (2) after non-uniform (localized) distribution of particles which are aligned along <100> is attained, the particle sizes become uniform, (3) the retardation of coarsening takes place.

Superalloys 1992
Edited by S.D. Antolovich, R.W. Stusrud, R.A. MacKay,
D.L. Anton, T. Khan, R.D. Kissinger, D.L. Klarstrom
The Minerals, Metals & Materials Society, 1992

Introduction

Recently, knowledge of the elasticity effects on precipitate morphology has rapidly been advancing. A typical example is the case in which the elastic interaction energy plays an essential role. A number of strange phenomena of coherent γ' precipitate particles (Ni_3X phase having an $L1_2$ structure) have been found one after another, *e.g.* the splitting of precipitate (1-6), the deceleration of precipitate coarsening (7-12), etc. Such strange phenomena can be understood only when the elasticity effect and, in particular, the effect of elastic interaction energy between particles are taken into consideration. The elastic interaction energy E_{int} originates from the overlap of the elastic strain fields around the individual coherent particles. An important feature of elastic interaction energy is that it has a negative minimum when the two particles are adjacent to each other along <100> directions (13).

Ardell, Nicholson and Eshelby (14) proposed an idea about the precipitate distribution. They showed that an elastic interaction between γ' particles actually arises from the difference between the elastic moduli of particle and matrix. Furthermore, they postulated that γ' particles become aligned along <100> directions due to the elastic interaction. Since then their conclusion has widely been recognized as describing the effect of elastic interaction on the two-phase microstructure containing coherent precipitates: *i.e.* the elastic interaction brings a fairly uniform (homogeneous) distribution of particles. However, a theoretical calculation by Doi, Fukaya and Miyazaki (15) predicted that the elastic interaction has a tendency to bring a non-uniform distribution of coherent particles. This prediction was proved by scanning electron microscopy of γ' particles in a Ni-Al-Ti alloy. The conclusion obtained by Doi et al. suggests that the already well-known idea proposed by Ardell et al. should be changed.

It is certain that a number of experimental studies published so far have discussed the directional distribution of precipitate particles in the course of ageing. However, since the distribution state cannot be expressed numerically, the discussion remains in a qualitative stage. The aims of the present study are (I) to propose two new parameters describing the state of particle distribution, (II) to observe with transmission electron microscopy (TEM) the distribution changes of coherent particles in Ni-base alloys, and (III) to discuss the elasticity effect on the precipitate distribution.

New Parameters Describing the Particle Distribution

A Parameter Describing the Directional Alignment

Fourier transformation of a two-phase structure containing precipitate particles gives a power spectrum containing information of the precipitate morphology. The area distant from the origin of the spectrum reflects the short-range correlation, *i.e.* the shape of the particles, while the area near the origin reflects the long-range correlation, *i.e.* the distribution of the particles. Figures 1-a and -b are schematic illustrations of two structures having the same morphology except for the particle shape. Figures 1-c and -d show the power spectra of the structures a and b, respectively. There is no practical difference between the two spectra in the intensity near the origin. Furthermore, satellites indicated by arrows can be seen in the spectra. The satellites for the two structures are the same. If the particles in a structure are aligned along a certain crystallographic direction [*hkl*], the intensity of the power spectrum of the structure increases in the [*hkl*] near the origin of the spectrum. Furthermore, if the particles are periodically arranged in the [*hkl*], satellites also appear in the [*hkl*]. The distance between the first satellite and the origin corresponds to the reciprocal of the mean inter-particle distance. The spectrum inside the circle whose radius is twice the distance between the first satellite and the origin (as shown schematically in Fig. 1-e) contains information only on the correlation larger than half of the mean inter-particle distance. Therefore, the spectrum inside the circle should be analyzed to eliminate the influence of particle shape.

To describe the degree of directional alignment of particles along [*hkl*], we define a new parameter Ψ_{hkl} as

$$\Psi_{hkl} \equiv (\psi_{hkl} - \psi_{min})/(\psi_{max} - \psi_{min}) \quad (1)$$

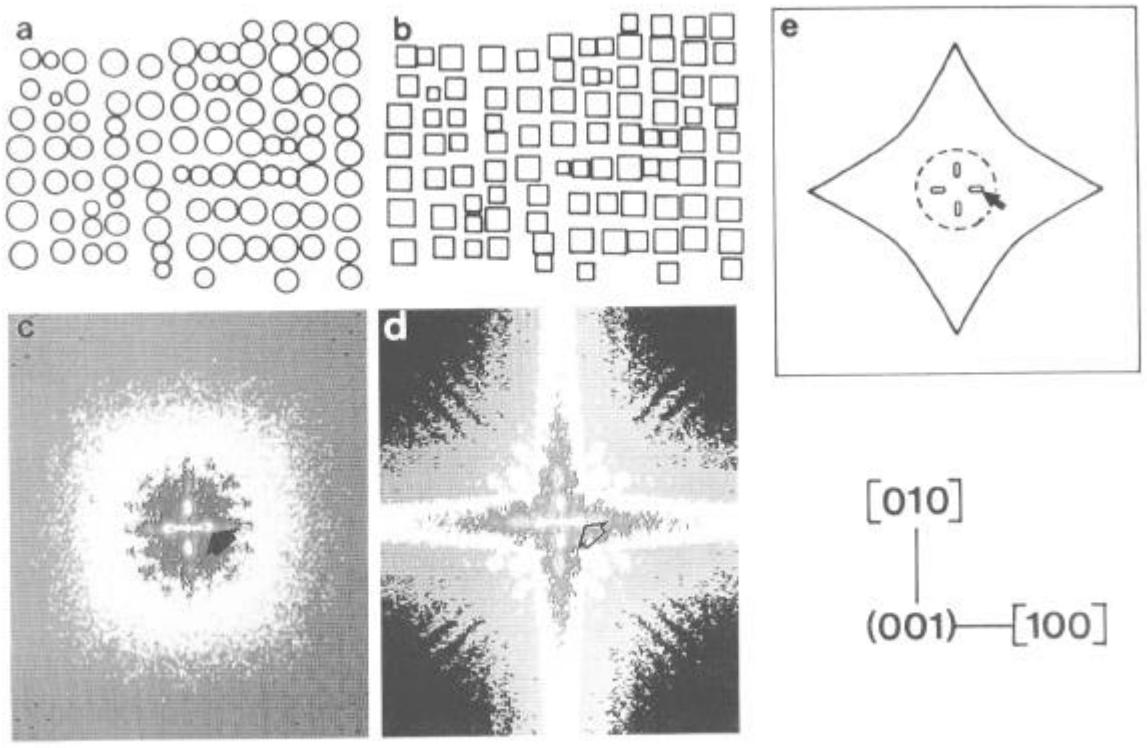

Figure 1 - Model structures (a,b), power spectra (c,d), and schematic illustration of the central part (near the origin) of the power spectrum d: c and d are obtained with Fourier transformation of a and b respectively.

Here ψ_{hkl} is given by

$$\psi_{hkl} = I_{hkl} / I_{all} \tag{2}$$

where I_{hkl} is the mean intensity of the power spectrum inside the circle in the [*hkl*] direction, and I_{all} is the mean intensity of the power spectrum inside the circle in all directions. Ψ_{min} is the Ψ value when particles are randomly distributed (without any directionality) and $\Psi_{min}=1$. Ψ_{max} is the ideal Ψ value when the distribution of particles is perfectly ordered. In Ni-base alloys containing coherent precipitate particles, Ψ_{100} is especially important because <100> directions are elastically soft.

Figure 2 illustrates TEM images of coherent Ni_3Mo particles in Ni-16.3at%Mo alloy aged at 973 K for 8.64×10^5 s (a) and for 2.59×10^6 s (c). At a glance, it seems that there is no practical difference between the two micrographs. However, we can recognize some difference between the power spectra of the structures (see Figs. 2-b and -d). The Ψ_{100} values are 0.0311 for the former and 0.0426 for the latter. The parameter Ψ_{hkl} can express the slight difference in the degree of particle alignment along [*hkl*]. Such a difference is not easily detected in TEM images.

A Parameter Describing the Non-uniform Distribution

When a square lattice is drawn on a micrograph of two-phase structure containing precipitate particles, the individual lattice points are on either the particle or the matrix, as illustrated in Fig. 3. The former points indicated by open circles are called P, while the latter points indicated by solid circles are called M. Here the lattice constant a_g is set to the mean particle size $2\bar{r}$ which corresponds to the inter-centre distance when the particles having the mean size are in contact with each other ($\bar{r}$ is the mean radius for spherical particles and mean half length of the edge of cuboidal particles). In Fig. 3, the nearest neighbour points can be described as three types of pairs: *i.e.* P–P, P–M and M–M. The more uniformly the particles are distributed, the larger the number of P–M pairs are. The more locally (non-uniformly) the particles are distributed forming groups, the larger the number of P–P and M–M pairs are. Therefore, the parameter λ which is defined by the following equation can describe the non-

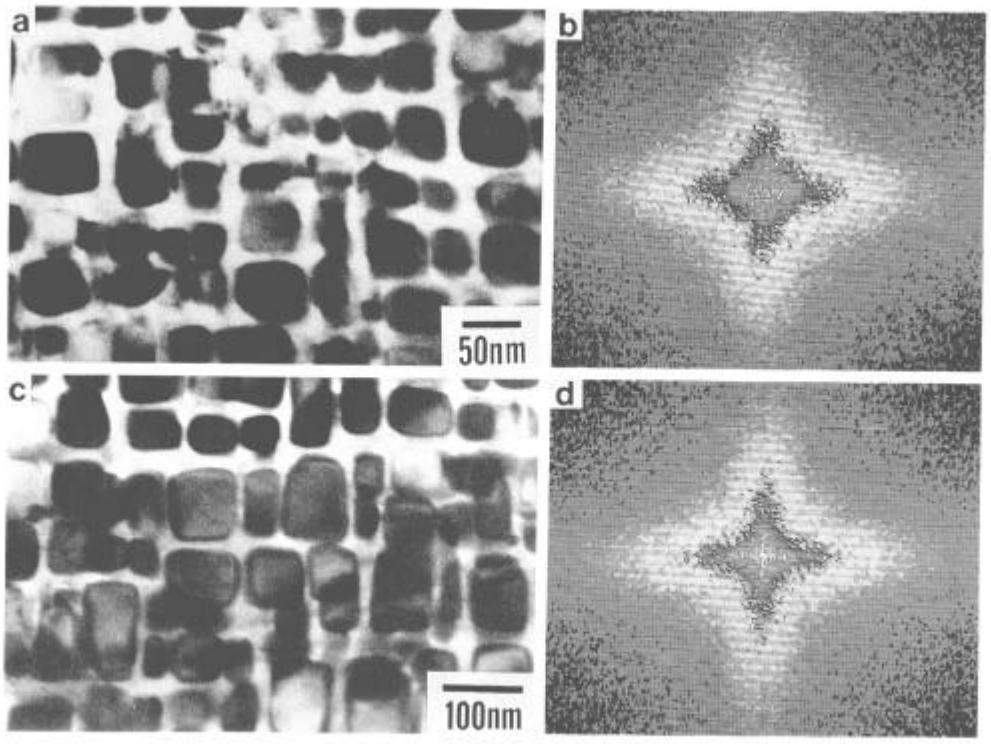

Figure 2 - TEM images and power spectra of Ni_4Mo particles in Ni-16.3at%Mo alloy aged at 973 K for 8.64 ks (a,b) and for 2.59 Ms (c,d).

uniformity in particle distribution:

$$\lambda = (n_{P-P} + n_{M-M} - n_{P-M})/n_{all} \tag{3}$$

where n_{X-Y} is the number of X–Y pair and n_{all} is the total number of all the pairs.

When the volume fraction of particles is not equal to 50 %, the value of n_{P-P} or n_{M-M} inevitably increases and hence the λ value also increases. Therefore, to eliminate such a shortcoming of λ, we must introduce a new parameter Λ defined as

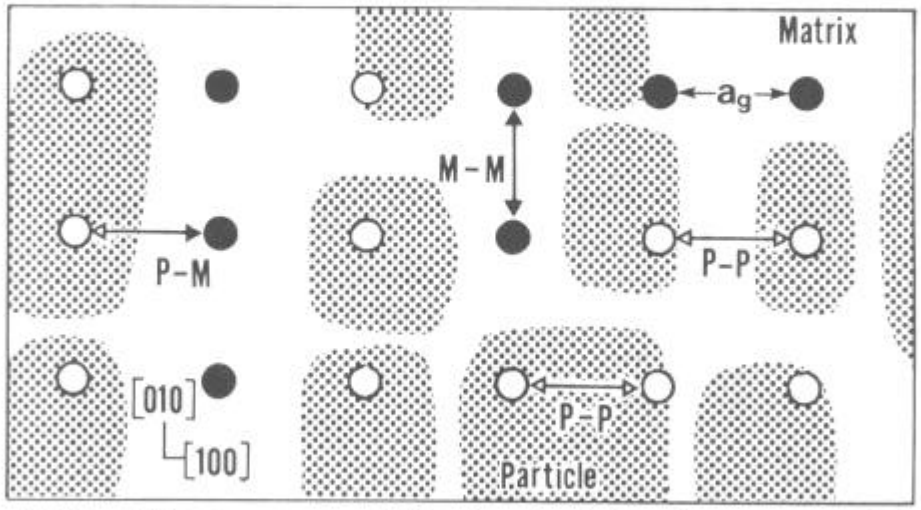

Figure 3 - A square lattice drawn on a model structure to calculate the parameter λ: the lattice points are indicated by the open circles (on particles) or the solid circles (on matrix).

$$\Lambda \equiv (\lambda - \lambda_{min})/(\lambda_{max} - \lambda_{min}) \quad (4)$$

λ_{min} is the minimum value of λ obtained when the particles are randomly distributed, and is given by

$$\lambda_{min} = A_f^2 + (1-A_f)^2 - 2A_f(1-A_f) \quad (5)$$

where A_f is the area fraction of particles, the first and the second terms express the probability of P-P and M-M pairs, and the third term expresses that of P-M pairs. λ_{max} is the maximum value of λ obtained when all the particles unite with each other to form a big square particle in the matrix, and is given by

$$\lambda_{max} = 1 - 2 \times \frac{2 \times 4 \times \sqrt{A_f \times 512 \times 400}/a_g}{2 \times (512/a_g - 1)(400/a_g - 1)} = 1 - \frac{160\, a_g \sqrt{2A_f}}{(32 - a_g)(25 - a_g)} \quad (6)$$

The numbers 512 and 400 appear because every micrograph to be analyzed is divided into 512 × 400 picture elements. By using the parameter Λ, we can correctly describe the degree of non-uniformity in particle distribution, *i.e.* the degree of localization of particles. For example, the Λ values for the structures in Figs. 2-a and -b are 0.103 and 0.272, respectively.

Quantitative Analyses of Morphological Changes in Elastically Constrained Systems

The distribution of coherent particles is greatly affected by the elastic interaction between particles. The elastic interaction arises from overlapping the elastic strain fields originated from lattice misfit δ between the particle and the matrix. The larger the δ is (*i.e.* the stronger the elastic constraint is), the stronger the effect of elastic interaction is. Furthermore, the elastic interaction is also a function of inter-particle distance and hence volume fraction f_v. To make clear the elasticity effect, particularly the effect of elastic interaction energy on the particle distribution, several Ni-base alloys having different δ and different f_v were used in the present study, as listed in Table I. The changes in particle distributions were observed with TEM and the changes were numerically analyzed by using the parameters Ψ_{100} and Λ explained in the previous section.

Table I Ni-Base Alloy Systems Used in the Present Study

Alloy System (at%)	Ageing Temperature T (K)	Lattice Misfit δ (%)	Volume Fraction f_v (%)
γ' / Ni-16.7Cr-6.1Al	1073	0.008	—
γ' / Ni-15.4Si	973	-0.30	33
γ' / Ni-14.0Al	973	0.56	25
γ' / Ni-14.0Al	1053	0.56	20
Ni_4Mo / Ni-16.3Mo	973	1.34	48
γ' / Ni-37.8Cu-5.5Si(Lf)	823	-1.29	20
γ' / Ni-36.2Cu-9.5Si(Hf)	823	-1.29	50

Weakly Constrained System

γ' in Ni-Cr-Al is typical of weakly constrained systems with very small $|\delta|$. In this system, the elasticity effect is negligibly small while the effect of surface energy is dominant. Figures 4-a and -b illustrate the TEM images of γ' particles in Ni-Cr-Al and the power spectra of the images. The power spectra exhibit neither directionality nor satellites. The changes in $\bar{r}$, Ψ_{100} and Λ during ageing are shown in Fig. 5 (•). Particle coarsening obeys the so-called $t^{1/3}$-law predicted by the LSW theory of

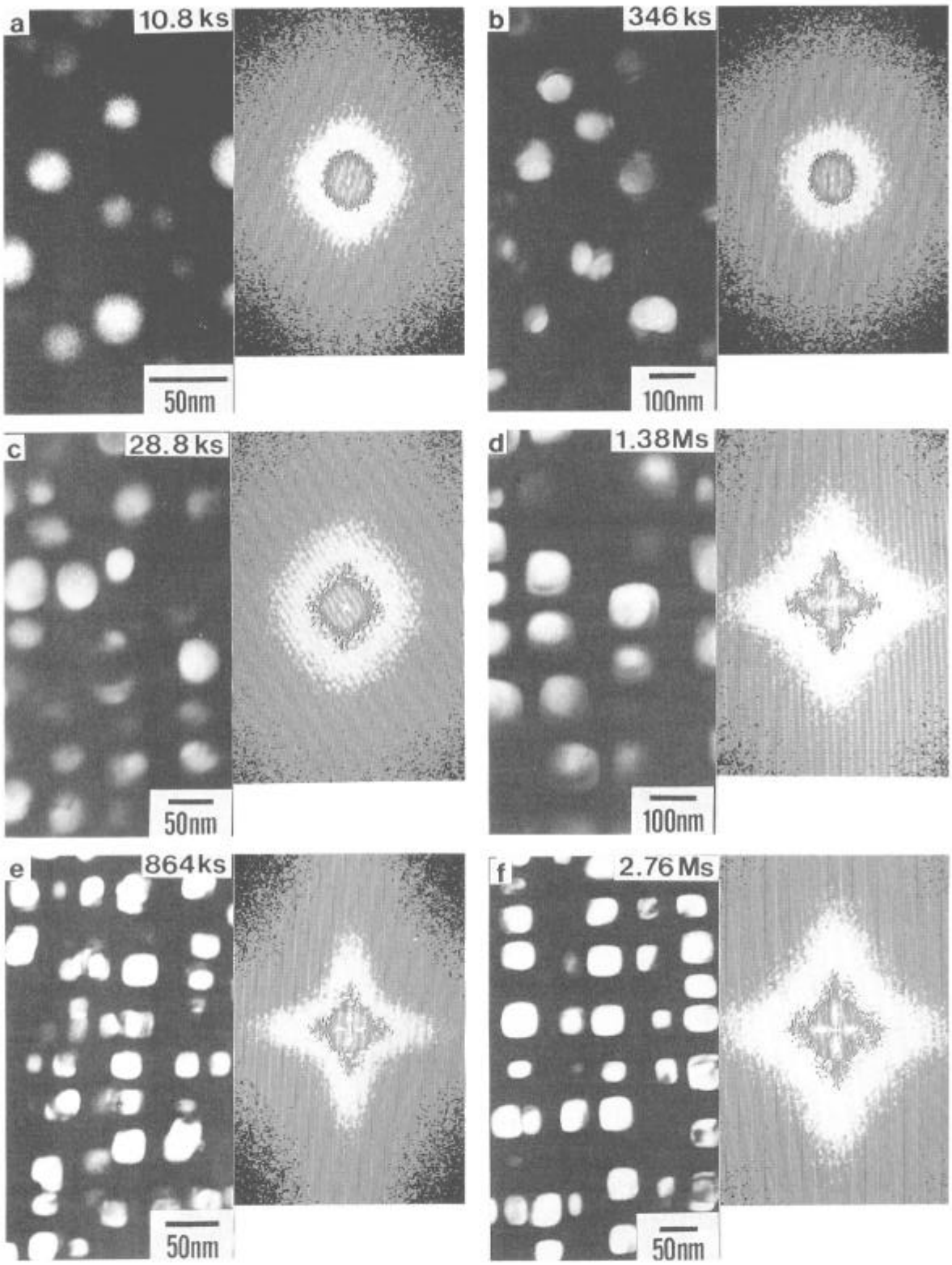

Figure 4 - TEM images and power spectra of γ' particles: Ni-16.7at%Cr-6.1at%Al aged at 1073 K (a,b); Ni-15.4at%Si aged at 973 K (c,d); Ni-37.8at%Cu-5.5at%Si(Lf) aged at 823 K (e,f).

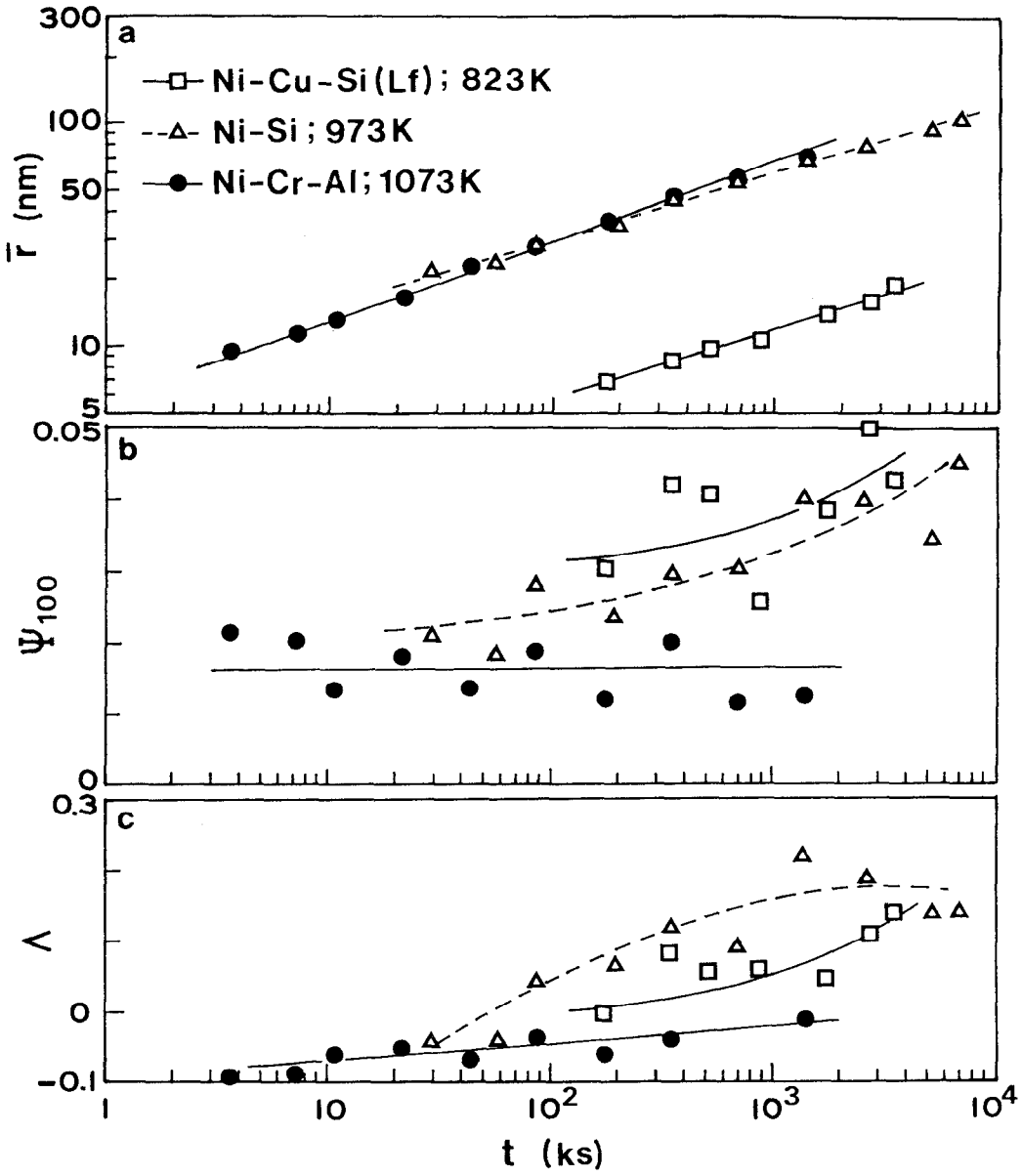

Figure 5 - Changes in $\bar{r}$, Ψ_{100} and Λ during ageing of Ni-base alloys.

Ostwald ripening. The values of Ψ_{100} and Λ remain small during ageing, which indicates that the particle distribution is quite uniform and exhibits no directional alignment.

Intermediately Constrained System

γ' in Ni-Si is typical of intermediately constrained systems with intermediate $|\delta|$. In this system, the elasticity effect is not dominant at smaller $\bar{r}$ but it becomes gradually stronger as particle coarsening proceeds. Figures 4-c and -d illustrate the TEM images of γ' particles in Ni-Si and the power spectra of the images. At the early stage of ageing, the power spectra exhibit neither obvious directionality nor satellites. However, as the ageing proceeds, directionality appears and the satellites become clear. The changes in $\bar{r}$, Ψ_{100} and Λ during ageing are shown in Fig. 5 (Δ). Particles coarsen slightly slower than the prediction of LSW theory. When $\bar{r}$ is small, Ψ_{100} is small and is similar to that of Ni-Cr-Al. Λ is also small at smaller $\bar{r}$. As coarsening proceeds, the system comes under the influence of elastic interaction because $|\delta|$ is rather large. γ' particles come to exhibit the alignment along <100> and the non-uniform (localized) distribution. Therefore, the values of Ψ_{100} and Λ increase. Similar behaviour is also observed for γ' particles in Ni-Al alloy. However, the elasticity effect in Ni-Al is

more obvious than that in Ni-Si because $|\delta|$ for Ni-Al is larger than that for Ni-Si.

Strongly Constrained System

γ' in Ni-Cu-Si is typical of strongly constrained systems having large $|\delta|$. Figures 4-e and -f illustrate the TEM images of γ' particles in Ni-Cu-Si(Lf) and the power spectra of the images. In this system, the elasticity effect appears even at the early stage of ageing because of large $|\delta|$. For example, satellites can clearly be seen in the power spectrum even at the early stage of ageing. This means that a good periodicity in particle distribution already exists due to elastic interaction between particles. The changes in $\bar{r}$, Ψ_{100} and Λ during ageing are shown in Fig. 5 (□). Coarsening proceeds more slowly than the prediction of LSW theory. The Ψ_{100} values are higher than other systems, which means that the tendency for particles to be aligned along <100> is stronger in Ni-Cu-Si as compared with other systems. This tendency is more obvious for Ni-Cu-Si(Hf) with high volume fraction than Ni-Cu-Si(Lf) with low volume fraction. Ni_4Mo in Ni-Mo is another system having large $|\delta|$. The ageing behaviour is similar to the case of γ' in Ni-Cu-Si. However, since the surface energy of Ni_4Mo in Ni-Mo is larger than that of γ' in Ni-Cu-Si, the elasticity effect is less dominant in Ni-Mo than in Ni-Cu-Si.

Elasticity Effect on the Particle Distribution

Figure 6-a illustrates the changes in Ψ_{100} of various systems as a function of $\bar{r}$. It can be seen from this figure that the larger the $|\delta|$ value is, the more smoothly the particles are aligned along <100> directions. When the lattice misfit is large, the elastic interaction energy is also large even at small $\bar{r}$ at

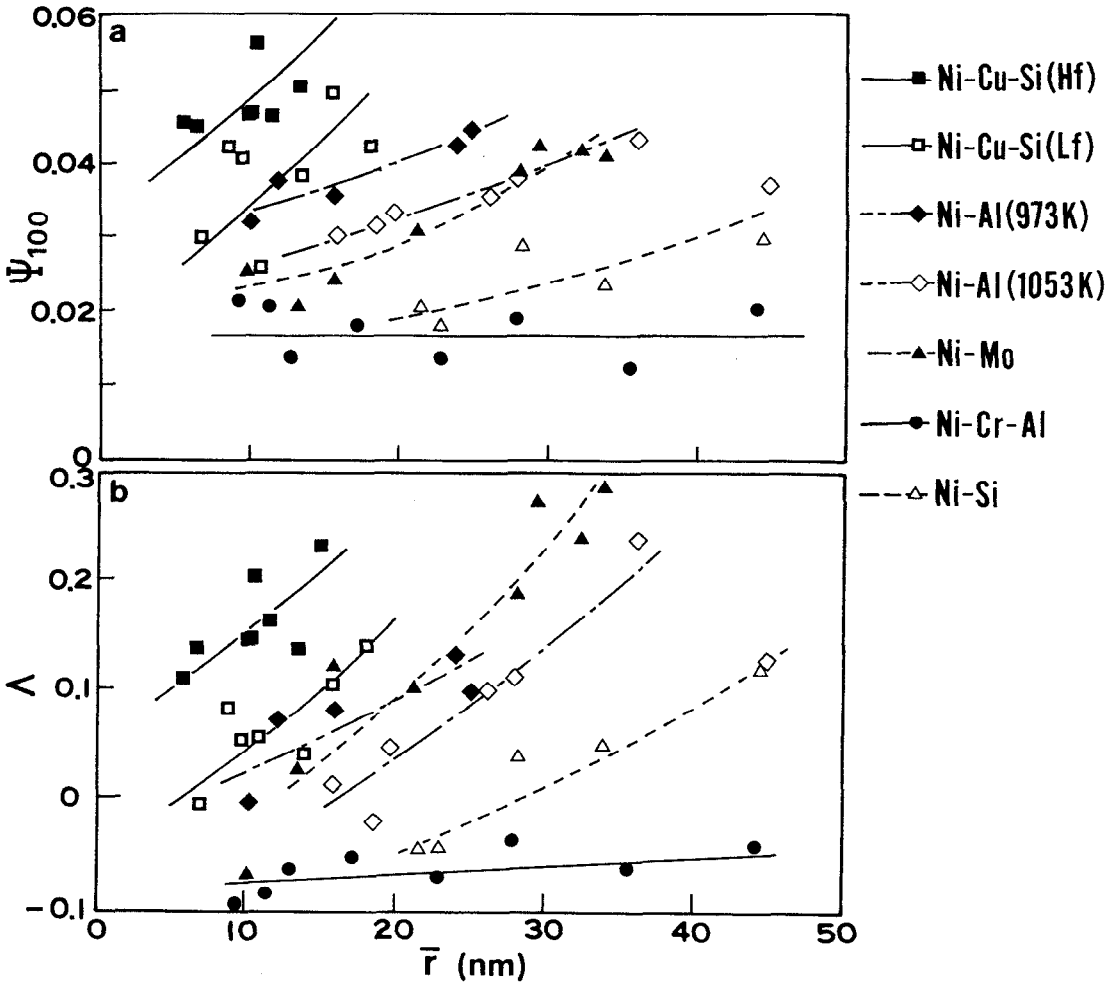

Figure 6 - Changes in Ψ_{100} and Λ for various Ni-base systems as a function of $\bar{r}$.

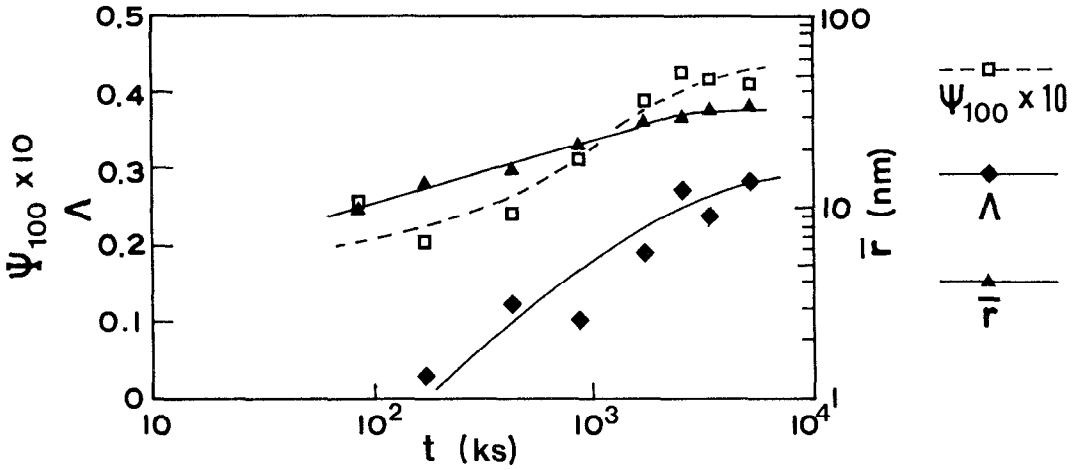

Figure 7 - Changes in $\bar{r}$, Ψ_{100} and Λ during ageing of Ni-16.3Mo at 973 K.

which, in general, the surface energy should be dominant. In such a case, the alignment along <100> is energetically favourable because the elastic interaction energy is negative in <100>. Therefore, when competitive growth takes place, the particles to be left are those aligned along <100> and the particles which are not aligned along <100> will disappear. Furthermore, when the $|\delta|$ value is large, the rate of alignment, *i.e.* $d\Psi/d\bar{r}$, is also large. The rate of alignment is roughly proportional to $|\delta|$: $d\Psi/d\bar{r} \sim 9.1\times10^{-4}|\delta|$.

Figure 6-a also indicates that the volume fraction of particles f_v affects the directional alignment. At a given $\bar{r}$, the Ψ value for the system having high volume fraction is larger than for the system having low volume fraction, although the volume fraction does not give any practical difference in the $d\Psi/d\bar{r}$ value. When the volume fraction is high, the inter-particle distance is short and hence the effect of elastic interaction is strong. Therefore, the particle alignment at high volume fraction is more susceptible to elastic interaction than that at low volume fraction.

Figure 6-b illustrates the changes in Λ of various systems as a function of $\bar{r}$. When $|\delta|$ is large, the Λ value is large at smaller $\bar{r}$ and the maximum of Λ value attained due to ageing is also large. The larger the $|\delta|$ value is, the more smoothly the Λ value increases. Furthermore, the system having higher volume fraction tends to exhibit larger Λ value. These results are natural because the non-uniform distribution of coherent particles arises from the elastic interaction energy.

Figure 7 illustrates the changes in $\bar{r}$, Ψ_{100} and Λ during ageing of Ni-Mo. At the early stage of coarsening, since the surface energy is dominant, precipitate particles are not localized and are not aligned along a certain direction. As coarsening proceeds, elasticity effect becomes dominant, and the particles begin to be aligned along <100> directions. A little later, the particles also begin to be localized thereby forming groups. Then non-uniform (localized) distribution of particles which are aligned along <100> is attained. And finally the particle sizes become uniform, which results in the retardation of coarsening. This kind of analysis has not been performed so far because we were unable to interpret the particle distribution numerically. It is clear that the parameters Ψ_{100} and Λ enable correct understanding of the sequence of morphological changes like the above.

Concluding Remarks

Many properties of Ni-base superalloys result from γ' precipitate morphology. Morphological changes of coherent particles are under the influence of elastic interaction between the particles. It is shown that two new parameters presented in this study are very useful to describe quantitatively the particle distribution. The morphological changes of precipitates like γ' can correctly be interpreted only by using the parameters. The sequence of the morphological changes of coherent particles under the influence of elastic interaction in Ni-base alloys is as follows: 1) alignment along <100>, 2) localization followed by group formation, 3) equalization of particle sizes, 4) retardation of coarsening.

Acknowledgements

The authors wish to thank Dr. T. Kozakai, Mr. T. Koyama and Mr. H. Okajima of Nagoya Institute of Technology for their co-operation. A part of this study was financially supported by a Grant-in-Aid for Scientific Research from the Ministry of Education, Science and Culture, Japan.

References

1. T. Miyazaki, H. Imamura, and T. Kozakai, "The Formation of "γ' Precipitate doublets" in Ni-Al alloys and their Energetic Stability," Materials Science and Engineering, 54 (1982), 9-15.

2. M. Doi, and T. Miyazaki, "The Effect of Elastic Interaction Energy on the Shape of γ'-Precipitate in Ni-Based Alloys," Superalloys 1984, ed. M. Gell et al. (Warrendale, PA: The Metallurgical Society, 1984), 543-552.

3. M. Doi, T. Miyazaki, and T. Wakatsuki, "The Effect of Elastic Interaction Energy on the Morphology of γ' Precipitates in Nickel-Based Alloys," Materials Science and Engineering, 67 (1984), 247-253.

4. M. Doi, T. Miyazaki, and T. Wakatsuki, "The Effects of Elastic Interaction Energy on the γ' Precipitate Morphology of Continuously Cooled Nickel-Base Alloys," Materials Science and Engineering, 74 (1985), 139-145.

5. M. J. Kaufman et al., "An Elastically Induced Morphological Instability of a Misfitting Precipitate," Metallurgical Transactions A, 20A (1989), 2171-2175.

6. Y. Wang, L.-Q. Chen, and A. G. Khachaturyan, "Shape Evolution of a Precipitate during Strain-Induced Coarsening," Scripta Metallurgica et Materialia, 25 (1991), 1387-1392.

7. W. C. Johnson, "On the Elastic Stabilization of Precipitates against Coarsening under Applied Load," Acta Metallurgica, 32 (1984), 465-475.

8. M. Doi et al., "Precipitate Coarsening under the Influence of Elastic Energy in Ni-Base Alloys," Dynamics of Ordering Processes in Condensed Matter, ed. S. Komura and H. Furukawa (New York: Plenum Press, 1988), 287-292.

9. M. Doi, and T. Miyazaki, "Microstructural Development under the Influence of Elastic Energy in Ni-Base Alloys Containing γ' Precipitates," Superalloys 1988, ed. S. Reichman et al. (Warrendale, PA: The Metallurgical Society, 1988), 663-672.

10. K. Kawasaki, and Y. Enomoto, "Statistical Theory of Ostwald Ripening with Elastic Field Interaction," Phisica A, 150 (1988), 463-498.

11. T. Miyazaki, and M. Doi, "Shape Bifurcations in the Coarsening of Precipitates in Elastically Constrained Systems," Materials Science and Engineering, A110 (1989), 175-185.

12. A. Onuki, and T. Nishimori, "Anomalously Slow Domain Growth due to a Modulus Inhomogeneity in Phase-Separating Alloys," Physical Review B, 43 (1991), 13649-13652.

13. T. Miyazaki et al., "Theoretical and Experimental Investigations on Elastic Interactions between γ'-Precipitates in a Ni-Al Alloy," Journal of Materials Science, 16 (1981), 1197-1203.

14. A. J. Ardell, R. B. Nicholson, and J. D. Eshelby, "On the Modulated Structure of Aged Ni-Al Alloys," with an Appendix "On the Elastic Interaction between Inclusions," Acta Metallurgica, 14 (1966), 1295-1309.

15. M. Doi, M. Fukaya, and T. Miyazaki, "Inhomogeneity in a Coherent Precipitate Distribution Arising from the Effects of Elastic Interaction Energies," Philosophical Magazine A, 57 (1988), 821-829.